Journal of Sound and Vibration (2001) **239**(4), 709–730
doi:10.1006/jsvi.2000.3224, available online at http://www.idealibrary.com on IDEAL®

THE ABSORPTION OF SOUND NEAR ABRUPT AXISYMMETRIC AREA EXPANSIONS

I. D. J. Dupère and A. P. Dowling

Cambridge University Engineering Department, Cambridge, CB2 1PZ, England

(*Accepted* 9 *August* 2000)

Sound incident onto an abrupt area expansion in an axisymmetric pipe is investigated analytically and experimentally. The incident sound field may synchronize the unsteady shedding of vorticity at the lip of the expansion to produce an organized train of vortices. In the presence of a mean flow, the unsteady vorticity shed from the lip is convected downstream where it acts as a sink or source of sound, thereby converting acoustic into vortical energy, or *vice versa*. An acoustic analogy and a Green function, G, are used to determine the sound reflected and transmitted across the area change. One finds that there is an optimal Strouhal number at which sound absorption is maximized and that this absorption can be enhanced by multiple reflections from the duct ends. In addition, the appropriate distance to be used in the definition of the Strouhal number depends upon the diameter ratio of the pipe expansion, $\lambda = a/b$, where a is the radius of the small pipe, and b is the radius of the larger pipe. For small λ, the appropriate length scale is the pipe radius, a; whereas for λ nearly equal to unity the appropriate length scale is the step height $b - a$. Predictions are compared with experiment.

© 2001 Academic Press

1. INTRODUCTION

Pipework systems of the type used in a car exhaust, or to transport water or natural gas, frequently involve the propagation of acoustic waves and a mean flow. At an abrupt increase in cross-sectional area of the pipe the mean flow separates, and there may be a coupling and energy exchange between the acoustic waves and vortical disturbances.

In his pioneering work on aerodynamic sound [1, 2], Lighthill considers the sound radiated from a region of non-linear fluid motion into an ambient fluid at rest, identifying the stress tensor, $T_{ij} = \rho u_i u_j + p_{ij} - c^2 \rho \delta_{ij}$, as a quadrupole source of aerodynamic sound. Here ρ is the fluid density, u_i is the component of the velocity in the i direction, p_{ij} is the compressive stress tensor, c is the ambient speed of sound and δ_{ij} is the Kronecker delta. In practice, however, the data required to calculate Lighthill's source term is difficult to obtain either by experiment or analytically, and alternative ways of writing the wave equation have been sought. After noticing that significant sound generation from steam locomotives is often accompanied by the formation of large eddies on the edge of the turbulent steam jet, Powell [3] introduced the concept of vortex sound. He identifies the Coriolis term, or vorticity impulse, $\nabla \cdot (\boldsymbol{\omega} \wedge \mathbf{u})$, as the most significant source of sound in low Mach number, high Reynolds number adiabatic flows. Here $\boldsymbol{\omega}$ represents the shed vorticity and $\mathbf{u}$ represents a flow velocity. This is a very attractive idea because it implies that the acoustic sources are confined to a region in which the vorticity is non-zero. This is a much smaller region than the one in which Lighthill's stress tensor, T_{ij}, is non-zero. Moreover, the data for the vorticity field is much easier to come by and can often be obtained from a simple

0022-460X/01/040709 + 22 $35.00/0 © 2001 Academic Press

analytical model, from computations or from experiment. Powell's justification, however, is not strict in terms of the acoustic analogy. More rigourous proofs are given by Howe and Doak [4–8] by reformulating the equations of motion (momentum and continuity) in terms of fluctuations in the stagnation enthaply, B, rather than fluctuations in either the pressure or the density. Both Howe and Doak argue that the Powell term, $(\boldsymbol{\omega} \wedge \mathbf{u})$ is the most significant source term in the low-speed, high Reynolds number, unheated flows.

Although Powell originally conceived the concept of vortex sound as a source description, the phase of its relationship to sound waves is often such that it acts as a sink rather than a source of sound. Indeed, it is well established that flows involving separation and vortex shedding can interact with incident acoustic waves, leading to acoustic absorption. Bechert [9] lists various devices which exploit this. As long ago as 1916, Borth [10] found that a throttle could dampen pressure oscillations in a duct. Frequently used devices for absorbing sound include orifice plates and perforated screens, and there vorticity is generated at the sharp edges of the apertures. When there is no mean flow, the fraction of incident energy absorbed depends non-linearly on the oncoming sound and high-amplitude acoustic waves are required before this mechanism of sound absorption is effective [11–14]. However, when there is a mean flow the sound absorption can be significant even for modest levels of excitation [15–17].

Whilst interaction between acoustic waves and vortical motion occurs in a wide range of problems of engineering interest, the influence of a mean flow on the transmission from the open end of a pipe has received the most attention. This is because of the importance of determining how much internal noise in a jet pipe of an aeroengine radiates to the far field. Carrier [18] extended Levine and Schwinger's classical result [19] for the radiation of internal sound from an open-ended pipe, to include the effects of the same uniform mean flow both inside and outside the pipe. Savkar [20] considered different internal and external mean flow velocities. He used an approximation to the Wiener–Hopf kernel and his solution has no instability waves. Munt [21, 22] obtains an exact solution to this problem. He applies the Kutta condition at the pipe exit and seeks a causal response to the incident sound wave. The mean velocity is assumed to be uniform in the jet issuing from the pipe, the jet being separated from the surrounding fluid by an infinitesimally thin shear layer. Such a shear layer is unstable and, according to Munt's theory, its instabilities are excited by an incident sound wave, leading to an external pressure field which grows exponentially with downstream distance within a region of, approximately, 45° to the downstream axis.

Cargill [23, 24] and Rienstra [25, 26] investigate the low-frequency limit of Munt's solution in some detail. For very low frequencies, the pressure reflection coefficient for incident plane waves in the jet pipe reduces to the no-flow reflection coefficient -1. Bechert [9] uses this as the basis of a simplified theory for finite Mach number, M, and low Helmholtz number, ka, where a is the radius of the jet pipe and $k = 2\pi f/c$ is the acoustic wavenumber for disturbances of frequency f. Rienstra [25] notes that there are two distinct low-frequency limits depending on the relative magnitudes of M and ka. For $ka \to 0$ with small non-zero M, the Strouhal number, $ka/\pi M$, tends also to zero and Levine and Schwinger's no flow result is recovered. In contrast, in the limit $M \to 0$ with small non-zero ka, the Strouhal number tends to infinity and a different end correction is predicted. This too is well confirmed experimentally [27]. Indeed, there is excellent agreement between Munt's theoretical reflection coefficient [22, 23, 25, 26] and experiments [27, 28].

Munt's theory is for jets with infinitesimally thin shear layers. Howe [29] overcomes the difficulties presented by the instability waves of such jets by a different approach, which is appropriate when the mean shear layer is thick in comparison with the viscous-controlled radial length scale $(\nu/2\pi f)^{1/2}$ of the unsteady vorticity shed from the nozzle lip (ν is the kinematic viscosity and $2\pi f$ is the radian frequency). Howe argues that, for linear

disturbances, the acoustic source term is $\nabla \cdot (\boldsymbol{\omega} \wedge \mathbf{u})$ [3–8], where $\boldsymbol{\omega}$, the vorticity shed at the jet lip, is chosen to satisfy the Kutta condition and is assumed to be subsequently convected away by the flow velocity $\mathbf{u}$. Although Howe's theory applies in the opposite physical limit from Munt's, i.e., for fairly thick rather than infinitesimally thin shear layers, the results are similar [29] if the direct contribution from the instability wave in Munt's solution is neglected. This may explain why Munt's reflection coefficient agrees well with experimental data for much thicker mean shear layers than the theory is valid [27].

Howe's approach had the advantage that it allows the Kutta condition to be imposed at a sharp edge in the presence of a mean flow without the introduction of exponentially large instability waves. The theory highlights the physics of the sound attenuation: acoustical energy is converted into kinetic energy of the unsteady vortical flow. The method has been applied to a range of problems including sound absorption by perforated plates [15–17, 30], slits [31–33] and sound production and absorption by Helmholtz resonators [34, 35] in the presence of either a normal or a tangential mean flow. It is found to agree well with experimental results.

In previous papers [36, 37], the problem of sound propagating past a two-dimensional backward facing step with a superimposed mean flow was considered. In those papers it was shown that, for sufficiently low Mach number, the simple analytical model developed by Howe [4, 15] gives acoustic absorption coefficients which agree well with experimentally determined values. In this paper, attention is given to the equivalent axisymmetric problem of linear absorption of sound by vortex shedding at an abrupt, axisymmetric area expansion in a pipe (where the pipe radius changes from a, in the smaller pipe, to b in the larger pipe). Both the Helmholtz number, ka, and the Mach number, M, are assumed low whilst the Strouhal number, $\mathrm{St}_a = af/\bar{u}$, is of order unity. Howe's theory is extended to this pipe geometry. Since the Helmholtz number is low, only plane waves propagate far upstream and far downstream of the expansion. For high Reynolds number flow, the main effects of viscosity are restricted to the region near the lip of the expansion, where the sound waves generate coherent unsteady vorticity. The strength of the shed vorticity is determined by applying the unsteady Kutta condition [38, 39] at the rim of the expansion, following the approach of Howe [15]. It is assumed that the amplitude of the incident sound wave is sufficiently small that any non-linearities can be neglected. This implies that strength of the unsteady shed vorticity depends linearly on the amplitude of the acoustic waves. It then convects downstream with the mean flow. The shed vorticity influences the unsteady flow through the expansion and thus alters the reflection and transmission of the incident sound waves. The shed vorticity is found to cause significant sound absorption for a range of Strouhal numbers. Initially, the absorption of sound is considered at a sudden expansion at the junction of two semi-infinite pipes with flow. In section 3, the analysis is extended to consider pipes of finite length. The validity of the theoretical solutions are tested by comparison with an experiment in section 4.

2. SEMI-INFINITE PIPES

Consider the pipework system shown in Figure 1. Two coaxial, semi-infinite pipes, of radii a and b, respectively, are aligned along the x-axis and joined at $x = 0$ (it is convenient to work in cylindrical polar co-ordinates (x, r, θ)). A high Reynolds number (based upon pipe diameter), low Mach number flow passes from the smaller to the larger diameter pipe. The mean flow separates at the lip of the expansion forming a jet downstream of the expansion. A low-amplitude incident plane sound wave of frequency, f, propagates from the left to the right towards the expansion at $x = 0$, where it is partly reflected and partly

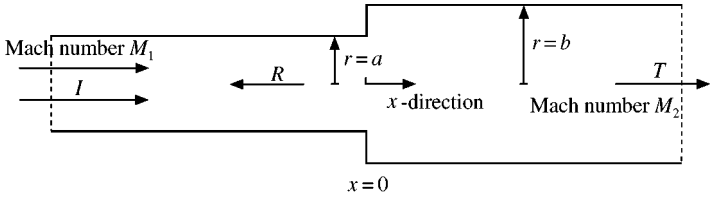

Figure 1. Axisymmetric pipe geometry.

transmitted into the larger diameter pipe. Unsteady vorticity is shed from the lip of the expansion by the sound waves and is subsequently convected downstream by the mean flow.

Following Doak and Howe [4–6, 8] the stagnation enthaply, B, is used as the dependent variable:

$$B = c_p T + \tfrac{1}{2}|\mathbf{u}|^2,$$

where T is the temperature and $\mathbf{u}$ is the fluid velocity. The sound field for each pipe will be considered separately and then matching conditions applied across the junction, $x = 0$, where $B' = B - \bar{B}(x, r)$ and $\partial B'/\partial x$ are continuous. Here the overbar denotes the mean value, and the prime denotes the perturbation. A similar approach has been used to investigate the transmission of sound through an orifice plate [40].

In Region 1 where $x < 0$, it is convenient to express the sound field as the superposition of the incident wave of amplitude B_0 in a pipe with a rigid end at $x = 0$, and a term $B^*(x, r)$, describing the additional contribution due to the pipe opening, i.e.,

$$B(x,r,t) = B_0\, \mathrm{e}^{-\mathrm{i}2\pi f(t - x/c(1+M_1))} + B_0\, \mathrm{e}^{-\mathrm{i}2\pi f(t + x/c(1-M_1))} + B^*(x,r)\, \mathrm{e}^{-\mathrm{i}2\pi f t} \quad \text{for } x < 0, \quad (1)$$

where M_1 is the mean flow Mach number far upstream of the expansion and c is the speed of sound. In the absence of any heating or flow inhomogeneities and ignoring the viscous terms and terms of order M^2, both B and B^* satisfy a convected wave equation in $y < 0$, where $\mathbf{y} = (y, r_0, \theta_0)$ is the position vector in cylindrical polar co-ordinates:

$$((1/c)\,\partial/\partial t + M_1\,(\partial/\partial y))^2\, B^* - \partial^2 B^*/\partial y_i^2 = 0 \quad \text{in } y < 0. \quad (2)$$

$B^*(y, r)$ depends upon the unsteady flow in the expansion and hence is coupled to the disturbances in the larger pipe. B^* can be related to this flow by introducing a Green function, $G_1(\mathbf{x}, t \,|\, \mathbf{y}, \tau)$, defined by

$$((1/c)\,\partial/\partial t + M_1\,(\partial/\partial y))^2\, G_1 - \partial^2 G_1/\partial y_i^2 = \delta(\mathbf{x} - \mathbf{y})\,\delta(t - \tau) \quad \text{in } y < 0, \quad (3)$$

where δ is the Dirac delta function. The choice of boundary conditions for G_1 is arbitrary and can be chosen to eliminate surface terms. Applying Green's theorem to equations (2) and (3) leads to

$$\mathrm{H}(-x_1)B^*(\mathbf{x},t) = \int_\tau \int_S \left(\frac{\partial G_1}{\partial \tau} \left(2\,\frac{M_1}{c}\,\delta_{1i} B^* + u_i \right) - B^*\,\frac{\partial G_1}{\partial y_i} \right) \mathrm{d}S_i\,\mathrm{d}\tau, \quad (4)$$

where S is a fixed control surface bounding the region $y < 0$ and H is the Heaviside function. It is convenient to choose the following set of boundary conditions G_1:

$$\partial G_1/\partial r_0 = 0 \quad \text{on } r_0 = a, \qquad \partial G_1/\partial y = 2\,(M_1/c)\,\partial G_1/\partial \tau \quad \text{on } y = 0, \tag{5, 6}$$

$$\text{inward behaviour as } y \to -\infty\,. \tag{7}$$

Equation (5) is chosen to eliminate contributions to the surface integral in equation (4) at the pipe walls (i.e., at $r_0 = a$), equation (6) eliminates contributions due to B^* at $y = 0$ (leaving contributions due only to **u**) whilst the choice of the farfield boundary condition is equation (7) which eliminates contributions from any outgoing acoustic waves to surface integrals at $y \to -\infty$. $G_1(\mathbf{x}, t \,|\, \mathbf{y}, \tau)$ has inward wave behaviour as $y_1 \to -\infty$ because it is a reciprocal Green function, whose source is at the observer's position $(\mathbf{x}, t)$. Inward wave behaviour in $(\mathbf{y}, \tau)$ leads to outward propagation in $(\mathbf{x}, t)$. With these boundary conditions equation (4) reduces to

$$B^*(\mathbf{x}, t) = -\int_\tau \int_0^a \left[\bar{G}_1 \frac{\partial u_1}{\partial \tau}\right] r_0\,\mathrm{d}r_0\,\mathrm{d}\tau, \tag{8}$$

where $\bar{G}_1(x, r, t \,|\, y, r_0, \tau) = \int_0^{2\pi} G_1(\mathbf{x}, t \,|\, \mathbf{y}, \tau)\,\mathrm{d}\theta$.

The Green function is calculated by using a Bessel series expansions. Write

$$\bar{G}_1(\mathbf{x}, t \,|\, \mathbf{y}, \tau) = \sum_{n=0}^{\infty} \int a_n(\mathbf{x}, t \,|\, y, f')\,\mathrm{J}_0(j_n r_0/a)\,\mathrm{e}^{\mathrm{i}2\pi f'\tau}\,\mathrm{d}f', \tag{9}$$

where J_0 is the Bessel function of order 0 and j_n denotes the nth zero J_1 i.e.

$$\mathrm{J}_1(j_n) = 0 \quad \text{for } n = 0, 1, 2, \ldots\,. \tag{10}$$

This expansion automatically satisfies boundary condition (5). The functions $a_n(\mathbf{x}, t \,|\, y, f')$ are determined by substitution of the series in equation (9) into equation (3).
The solution follows a very similar approach to that for the equivalent boundary conditions in the two-dimensional problem [37]. The result is

$$a_n(\mathbf{x} | y, \theta) = \frac{\mathrm{i}\mathrm{J}_0(j_n r_0/a)}{a^2(\delta_n)\mathrm{J}_0^2(j_n)}\,\mathrm{e}^{-\mathrm{i}(2\pi f t - kM_1(y - x))} \times \left(\mathrm{e}^{\mathrm{i}\delta_n|x - y|} - \left(\frac{kM_1 - \delta_n}{\delta_n + kM_1}\right)\mathrm{e}^{-\mathrm{i}\delta_n(x + y)}\right) \quad \text{for } x, y < 0. \tag{11}$$

Substitution of the expansion for $B^*(y)$ in equation (8) into equation (1) yields

$$B(x, r) = B_0\,\mathrm{e}^{\mathrm{i}kx/(1 + M_1)} + B_0\,\mathrm{e}^{-\mathrm{i}kx/(1 - M_1)} - \int_{-\infty}^{\infty} \int_0^a \bar{G}_1\,\mathrm{e}^{\mathrm{i}2\pi f t}\,\frac{\partial u_1}{\partial \tau}\,(0, r_0) r_0\,\mathrm{d}r_0\,\mathrm{d}\tau. \tag{12}$$

It is convenient to introduce a function $U(r_0)$ to describe the axial velocity fluctuations through the junction. Then, since all the flow parameters have time dependence $\mathrm{e}^{-\mathrm{i}2\pi f\tau}$, i.e., are periodic with frequency f, we have

$$(\partial u_1/\partial \tau)\,(0, r_0, \tau) = -\mathrm{i}2\pi f U(r_0)\mathrm{e}^{-\mathrm{i}2\pi f\tau}. \tag{13}$$

Substituting into equation (12) gives

$$B(x, r) = B_0\,\mathrm{e}^{\mathrm{i}kx/(1+M_1)} + B_0\,\mathrm{e}^{-\mathrm{i}kx/(1-M_1)} + \int_{-\infty}^{\infty}\int_0^a \mathrm{i}2\pi f \bar{G}_1\, U(r_0)\mathrm{e}^{\mathrm{i}2\pi f(t-\tau)} r_0\,\mathrm{d}r_0\,\mathrm{d}\tau. \quad (14)$$

Equation (14) is a general equation relating the stagnation enthalpy in the first pipe to the (known) Green function and the (as yet unknown) function $U(r_0)$. This function is to be found by considering the flow in the second pipe ($x > 0$) and using the fact that all flow variables are to be continuous at the pipe expansion, $x = y = 0$.

Downstream of the expansion there is vorticity (which is shed from the lip of the expansion) which acts as an acoustic source term in equation (2). The equation for the sound field in the larger pipe therefore becomes (neglecting terms of order M in this very low Mach number flow) [37]

$$((1/c)\,\partial/\partial t + M_2\,(\partial/\partial y))^2\; B - \partial^2 B/\partial y_i^2 = (\partial/\partial y_i)\,(\boldsymbol{\omega} \wedge \mathbf{u})_i, \quad (15)$$

where $M_2 = M_1 a^2/b^2$. Since the mean flow separates at $y = 0$, M_2 is not the mean flow Mach number at the locations near $y = 0$ where the flow separates, but only as $y \to -\infty$.

Once again the solution is obtained by introducing a Green function $G_2(\mathbf{x}\,|\,\mathbf{y})$, which is defined as

$$((1/c)\,\partial/\partial t + M_2\,(\partial/\partial y))^2\, G_2 - \partial^2 G_2/\partial y_i^2 = \delta(\mathbf{x} - \mathbf{y})\delta(t - \tau). \quad (16)$$

The boundary conditions are equivalent to those used in the smaller pipe:

$$\partial G_2/\partial r_0 = 0 \quad \text{on } r_0 = b, \qquad \partial G_2/\partial y = 2\,(M_2/c)\,\partial G_2/\partial \tau \quad \text{on } y = 0, \quad (17, 18)$$

$$\text{inward behaviour as } y \to \infty \quad (19)$$

The solution for the Green function in the larger pipe is

$$\bar{G}_2 = \int G\,\mathrm{d}\theta, \quad (20)$$

$$\bar{G}_2(\mathbf{x}, t\,|\,\mathbf{y}, \tau) = \sum_{n=1}^{\infty} \int b_n(\mathbf{x},\, t|\mathbf{y}, f')\mathrm{J}_0(j_n r_0/b)\,\mathrm{e}^{\mathrm{i}2\pi f'\tau}\,\mathrm{d}f', \quad (21)$$

$$b_n = \frac{\mathrm{i}\mathrm{J}_0(j_n r_0/b)}{b^2\gamma_n \mathrm{J}_0^2(j_n)}\,\mathrm{e}^{-\mathrm{i}(2\pi f t - kM_2(y-x))}\left(\mathrm{e}^{\mathrm{i}\gamma_n|x-y|} + \left(\frac{kM_2 + \gamma_n}{\gamma_n - kM_2}\right)\mathrm{e}^{\mathrm{i}\gamma_n(x+y)}\right), \quad (22)$$

where $\gamma_n = \sqrt{k^2 - (j_n/b)^2}$. The imaginary part of γ_n is taken as being positive if γ_n is complex. Applying Green's second theorem and the boundary conditions, as before, gives

$$B(x,r)\,\mathrm{e}^{-\mathrm{i}2\pi f t} + \int\int\int G_2\,\boldsymbol{\nabla}\cdot(\boldsymbol{\omega} \wedge \mathbf{u})\mathrm{d}^3 y\,\mathrm{d}\tau = \int_{-\infty}^{\infty}\int_0^b \bar{G}_2\,\frac{\partial u_i}{\partial \tau}(0, r_0)\,r_0\,\mathrm{d}r_0\,\mathrm{d}\tau$$

$$= -\,\mathrm{i}2\pi f \int_{-\infty}^{\infty}\int_0^a \bar{G}_2\,U(r_0)\mathrm{e}^{-\mathrm{i}2\pi f r}\,r_0\,\mathrm{d}r_0\,\mathrm{d}\tau \quad (23)$$

in $y > 0$. Note that the integral in the last term in equation (23) is from $r_0 = 0$ to a because $U(r_0)$ is zero on the rigid wall from a to b.

For a mean flow with a shear layer which is thick in comparison with the viscous-controlled radial length scale $(\nu/2\pi f)^{1/2}$ of the unsteady vorticity shed from the rim of the expansion; the vorticity source term $\nabla\cdot(\boldsymbol{\omega}\wedge\mathbf{u})$ can be calculated by following the procedure of Howe [15, 29]. After linearization,

$$\nabla\cdot(\boldsymbol{\omega}\wedge\mathbf{u})' = \nabla\cdot(\boldsymbol{\omega}'\wedge\bar{\mathbf{u}}) + \nabla\cdot(\bar{\boldsymbol{\omega}}\wedge\mathbf{u}'), \tag{24}$$

where the overbar denotes the mean value and the prime denotes a perturbation. Howe assumes that the sound field resulting from the second term on the right side of equation (24) is small in comparison with the first term. In the equivalent two-dimensional problem [36, 37] a numerical solution was used to confirm the validity of this approximation.

As in the two-dimensional problem [36, 37], it is assumed also that the unsteady vorticity which is shed from the rim of the expansion forms an infinitesimally thin shear layer which convects downstream with mean flow velocity $\mathbf{u}_c = (\bar{u}_c, 0, 0)$ where $\bar{u}_c$ is typically about half the jet exist velocity. This assumption is reasonable given the previous assumption that the acoustic shear layer is thin compared with the mean shear layer. The unsteady vorticity, $\boldsymbol{\omega}'$, is therefore written in the form

$$\boldsymbol{\omega}' = \sigma\,\mathrm{H}(y)\delta(r_0 - a)\mathrm{e}^{\mathrm{i}(\kappa y - 2\pi f\tau)}\mathbf{e}_\theta, \tag{25}$$

where σ denotes the strength/unit length of the vortex sheet, and again $\kappa = 2\mathrm{n}f/\bar{u}_c$, $\mathrm{H}(y)$ is the Heaviside function and $\mathbf{e}_\theta$ is a unit vector in the azimuthal direction.

One can substitute for $\boldsymbol{\omega}'$ in equation (23) from equation (25) to give, after integration

$$B(x,r) + \sigma S(x,r) = -\,\mathrm{i}2\pi f\int_{-\infty}^{\infty}\int_0^a \bar{G}_2 U(r_0)\mathrm{e}^{\mathrm{i}2\pi f(t-\tau)} r_0\,\mathrm{d}r_0\,\mathrm{d}\tau, \tag{26}$$

where

$$S(x,r) = -\int\int\sum_{n=1}^{\infty}\frac{\mathrm{J}_0(j_n r/b) a j_n U_0 \mathrm{J}_1(j_n\lambda)(kM_2+\gamma_n)}{b^3\gamma_n \mathrm{J}_0^2(j_n)(\kappa^2-\gamma_n^2)(\gamma_n - kM_2)}$$
$$\times(2(\kappa-\gamma_n)\mathrm{e}^{-\mathrm{i}\kappa M_2 x}\cos(\gamma_n x) - \gamma_n \mathrm{e}^{\mathrm{i}\kappa x})\,\mathrm{d}f'\,\mathrm{e}^{\mathrm{i}2\pi(f-f')\tau}\,\mathrm{d}\tau \tag{27}$$

and $\lambda = a/b$. The unknown function, $U(r_0)$, is to be determined from the matching condition that $B(y, r_0)$ is continuous across $y = 0$, $r_0 < a$. Application of this condition to equations (14) and (26) leads to

$$B(0,r) = 2B_0 + \int_0^a \mathrm{i}2\pi f g_1 U(r_0) r_0\,\mathrm{d}r_0 = -\int_0^a \mathrm{i}2\pi f g_2 U(r_0) r_0\,\mathrm{d}r_0 - \sigma S(x,r), \tag{28}$$

where

$$g_1(r|r_0) = \int_{-\infty}^{\infty}\bar{G}_1(0,r,t|0,r_0,\tau)\mathrm{e}^{\mathrm{i}2\pi f(t-\tau)}\,\mathrm{d}\tau$$

and

$$g_2(r|r_0) = \int_{-\infty}^{\infty}\bar{G}_2(0,r,t|0,r_0,\tau)\mathrm{e}^{\mathrm{i}2\pi f(t-\tau)}\,\mathrm{d}\tau.$$

For a general value of σ, $B(0, r_0)$ has a singularity of the form $(1 - r_0/a)^{-1/3}$ near the edge $r_0 = a$. The unsteady Kutta condition requires that the flow remain finite everywhere and so

a specific value of σ is obtained. In order to apply this condition, $U(r)$ is separated into a component $B_0V(r_0)$ due to the oncoming sound and a component $\sigma W(r_0)$ due to the vorticity by writing

$$U(r_0) = B_0V(r_0) + \sigma W(r_0). \tag{29}$$

Thus, equation (28) becomes

$$-\int_0^a (g_1 + g_2)\mathrm{i}2\pi f(B_0V(r_0) + \sigma W(r_0))r_0\,\mathrm{d}r_0 = 2B_0 + \sigma S(r, 0) \quad \text{for } r_0 \leqslant a. \tag{30}$$

Equation (30) can be decoupled into two equations (one for the oncoming sound contribution, and one for the vorticity contribution):

$$-\int_0^a (g_1 + g_2)\mathrm{i}2\pi f V(r_0)r_0\,\mathrm{d}r_0 = 2, \tag{31}$$

$$-\int_0^a (g_1 + g_2)\mathrm{i}2\pi f W(r_0)r_0\,\mathrm{d}r_0 = S(r, 0). \tag{32}$$

The two unknown functions, $V(r_0)$ and $W(r_0)$, are now determined by expanding them as series of Bessel functions and making use of the known form of the singularities in $V(r_0)$ and $W(r_0)$ ($V(r_0)$, $W(r_0) \to (1 - r_0/a)^{-1/3}$ as $r_0 \to a$) by writing

$$(1 - r_0/a)^{1/3}\,V(r_0) = \sum_{m=0}^{\infty} V_m \mathrm{J}_0(j_m r_0/a) \tag{33}$$

and

$$(1 - r_0/a)^{1/3}\,W(r_0) = \sum_{m=0}^{\infty} W_m \mathrm{J}_0(j_m r_0/a). \tag{34}$$

The unknown coefficients, V_m and W_m, are found by substituting equations (33) and (34) into equations (31) and (32), respectively, and using the orthogonality property of the Bessel functions. Before doing this, however, it is convenient to introduce the following non-dimensional variables:

$$r_0' = r_0/a, \qquad r' = r/a, \qquad \gamma_n' = a\gamma_n \quad \text{and} \quad \delta_n' = a\delta_n. \tag{35}$$

Rewriting equations (14) and (26) in terms of these variables makes it apparent that the reflection and transmission of the acoustic waves depends upon $\kappa a(= 2\pi f a/U_c)$, $ka(= 2\pi f a/c)$ and the diameter ratio $\lambda(= a/b)$.

Substitution of equation (33) into equation (31) then gives

$$2 = \sum_{m,n=0}^{\infty} \frac{\kappa a U_c V_m \mathrm{J}_0(j_n r')}{\mathrm{J}_0^2(j_n)(\delta_n')} \int_0^1 (1 - r_0')^{-1/3}\mathrm{J}_0(j_n r_0')\mathrm{J}_0(j_m r_0')r_0'\,\mathrm{d}r_0'$$
$$+ \sum_{m=n=0}^{\infty} \frac{\kappa a \lambda^2 U_c V_m \mathrm{J}_0(j_n \lambda r')}{\mathrm{J}_0^2(j_n)(\gamma_n)} \int_0^1 (1 - r_0')^{-1/3}\mathrm{J}_0(j_n \lambda r_0')\mathrm{J}_0(j_m r_0')r_0'\,\mathrm{d}r_0'. \tag{36}$$

After multiplying through by $r'\mathrm{J}_0(j_p r')$ and integrating with respect to r', the orthogonality of the Bessel functions [41] can be used to show that

$$\sum_{m=0}^{\infty} X_{pm} V_m U_c = \delta_{p0} \quad \text{for } p = 0, 1, 2, \ldots, \tag{37}$$

where

$$X_{pm} = \frac{\kappa a}{(2\gamma'_n)} \int_0^1 (1 - r'_0)^{-1/3} \, \mathrm{J}_0(j_n r'_0) \mathrm{J}_0(j_m r'_0) r'_0 \, \mathrm{d}r'_0$$

$$+ \sum_{n=0}^{\infty} \frac{\kappa a \lambda^2 U_c V_m I_{pn}}{\mathrm{J}_0^2(j_n)\gamma'_n} \int_0^1 (1 - r'_0)^{-1/3} \, \mathrm{J}_0(j_n \lambda r'_0) \mathrm{J}_0(j_m r'_0) r'_0 \, \mathrm{d}r'_0 \tag{38}$$

and

$$I_{pn} = \int_0^1 \mathrm{J}_0(j_p r'_0) \mathrm{J}_0(j_n \lambda r'_0) r'_0 \, \mathrm{d}r'_0. \tag{39}$$

Likewise substitution for $W(r)$ from equation (34) into equation (32) yields

$$\sum_{m=0}^{\infty} X_{pm} W_m = Y_p \quad \text{for } p = 0, 1, 2, \ldots, \tag{40}$$

where Y_p is given by

$$Y_p = -2 \sum_{n=0}^{\infty} \frac{\lambda^3 j_n U_c \mathrm{J}_1(j_n \lambda) I_{pn} (kaM_2 + \gamma'_n)(kaM_2 - 2\gamma'_n + \kappa a)}{(\gamma'_n)(\kappa^2 a^2 - \gamma'^2_n)(\gamma'_n - kaM_2)\mathrm{J}_0^2(j_n)}. \tag{41}$$

Equations (37) and (40) need to be solved numerically and so truncation is necessary. The summation over n in X_{pm} is truncated at the Nth term, where typically $N = 500$. Extensive checks were made to ensure that the results were independent of N. The sum over m is truncated after $(M + 1)$ terms, and then the first $(M + 1)$ equations (37) and (40) are solved using Crout's factorization with partial pivoting. The integrals are evaluated numerically using an adaptive integrator which is particularly suitable for oscillating integrands.

Having found the coefficients V_m, $m = 0, \cdots, M$, and W_m, $m = 0, \cdots, M$, the Kutta condition is applied so as to relate the shed vorticity strength, σ, to the incident sound wave, B_0. After substituting for $V(r)$ and $W(r)$ from equations (33) and (34) into equation (29), the requirement that $U(r)$ remains finite as $r \to a$ gives

$$\sigma = -\frac{B_0 \sum_{m=0}^{M} V_m \mathrm{J}_0(j_m)}{\sum_{m=0}^{M} W_m \mathrm{J}_0(j_m)}. \tag{42}$$

The stagnation enthalpy far upstream and far downstream of the expansion then follows from the substitution of the now known function $U(r)$ into equations (14) and (26). For low-frequency waves for which $kb < j_1 = 3{\cdot}832$, all values of δ_n, with the exception of $\delta_0 = k$ are imaginary and so the waves decay exponentially. Hence the pipe modes are "cut-off". Thus the expressions for the sound field, $B(x)$, away from the expansion simplify greatly, leaving only the $n = 0$ terms and a contribution from the vorticity source term. Far upstream

$$B(x) = B_0 \, \mathrm{e}^{\mathrm{i}kx/(1 + M_1)} + B_0 \mathrm{e}^{-\mathrm{i}kx/(1 - M_1)}$$

$$- \mathrm{e}^{-\mathrm{i}kx/(1 - M_1)} c \sum_{m=0}^{M} \left(\frac{B_0 V_m + \sigma W_m}{1 + M_1} \right) \int_0^1 (1 - r'_0)^{-1/3} \mathrm{J}_0(j_m r'_0) r'_0 \, \mathrm{d}r'_0. \tag{43}$$

Similarly, far downstream

$$B(x) = \mathrm{e}^{\mathrm{i}kx/(1+M_2)}\, c\lambda^2 \sum_{m=0}^{M} \left(\frac{B_0 V_m + \sigma W_m}{1-M_2}\right) \int_0^1 (1-r_0')^{-1/3} \mathrm{J}_0(j_m r_0') r_0' \,\mathrm{d}r_0'$$

$$+ \mathrm{e}^{\mathrm{i}\kappa x}\, \sigma \sum_{n=1}^{\infty} \frac{-\mathrm{J}_0(j_n r')\lambda^3 j_n U_c \mathrm{J}_1(j_n\lambda)(kaM_2 + \gamma_n')}{(\gamma_n')\mathrm{J}_0^2(j_n)\ (\gamma_n' - kaM_2)}. \tag{44}$$

The last term in equation (44) above describes the enthalpy generated directly by the shed vorticity. This is a factor $(\sigma U_c/B_0)\ M^2/\kappa a$ smaller than the other term. $\sigma U_c/B_0$ is at most 5×10^{-3} and so $(\sigma U_c/B_0)\ M^2/\kappa a < 10^{-3}$ for all values of κa greater than 0·02 for the range of Mach numbers considered. Hence, the last term may be safely neglected.

Whilst the distant sound fields can be determined directly from equations (43) and (44), the calculations involved are extremely time consuming. It is found that a greater number of terms in the series are required than are needed to solve for the vorticity strength, σ. Instead of following this approach, therefore, it is quicker to use a different Bessel series expansion for $U(r_0)$, exploiting the fact that, for the vorticity strength calculated in equation (42), $U(r_0)$ is now finite as $r \to a$. Hence, we expand

$$U(r_0) = B_0 \sum_{m=0}^{\infty} U_m \mathrm{J}_0(jm\, r_0/a) \tag{45}$$

and substitute into equation (28). Multiplying through by $r_0'\mathrm{J}_0(j_p r_0')$ and integrating with respect to r_0' leads to

$$\frac{1}{U_c}\,\delta_{p0} - \kappa a\, \frac{\mathrm{J}_0^2 j_p}{4\gamma_n'} = \sum_{m=n=0}^{\infty} \frac{\kappa a \lambda^2 U_c V_m I_{pn} I_{mn}}{\mathrm{J}_0^2(j_n)\,\gamma_n'}. \tag{46}$$

Again this is solved by truncating the sums over m and n at M and N, respectively, and using the first $(M+1)$ equations to determine the coefficients U_m, $m = 0, \cdots, M$. These coefficients have more physical meaning than those in equation (43), since they represent the different acoustics modes of the pipe. In particular, $m = 0$ is the plane wave mode. Thus, far upstream of the expansion the sound field is given by

$$B(x) = B_0(\mathrm{e}^{\mathrm{i}kx/(1+M_1)} + \mathrm{e}^{-\mathrm{i}kx/(1-M_1)}\,(1 - (cU_0/(1+M_1)))), \tag{47}$$

whilst far downstream we have

$$B(x) = B_0 \mathrm{e}^{\mathrm{i}kx/(1+M_2)}\,(c\lambda^2 U_0/(1-M_2)). \tag{48}$$

Equations (47) and (48) only involve U_0, the first coefficient in the expansion for $U(r)$ representing the planar mode. U_0 depends only weakly on the subsequent terms in the expansion and $M = 50$ is found to be sufficiently large to determine U_0 to three significant figures.

Having determined the distant sound fields upstream and downstream of the expansion, the acoustic absorption coefficient, Δ, the absorbed energy as a fraction of the incident sound energy, is calculated:

$$\Delta = \frac{\text{Incident energy} - \text{outgoing energy}}{\text{Incident energy}} = \frac{I_{in}A_1 - (I_r A_1 + I_t A_2)}{I_{in}A_1}, \tag{49}$$

where I is the intensity and the suffices *in*, *r* and *t* denote the incident, reflected and transmitted sound waves respectively; and $A_1 = \pi a^2$ and $A_2 = \pi b^2$ are the areas of the ducts upstream and downstream of the expansion respectively. The magnitudes of the acoustic intensities are given by [42] $I = |(p' + \bar{\rho}\mathbf{v}\cdot\mathbf{v}')(\mathbf{v}' + (p'\mathbf{v}))/(\bar{\rho}\bar{c}^2)|$, which in terms of the wave amplitudes is

$$I_{in} = (p'^2_{in}/\rho c)(1 + M_1)^2 = B'^2_{in}\ \rho/c, \qquad I_r = (p'^2_r/\rho c)(1 - M_1)^2 = B'^2_r \rho/c, \quad (50, 51)$$

$$I_t = (p'^2_t/\rho c)(1 + M_2)^2 = B'^2_t\ \rho/c, \quad (52)$$

where p' is the acoustic pressure and B' is the acoustic stagnation enthalpy. Thus,

$$\Delta = \frac{B'^2_{in} - B'^2_r - B'^2_t \lambda^2}{B'^2_{in}} \quad (53)$$

$$= 1 - \left|1 - \left(\frac{c}{1 + M_1}\right)U_0\right|^2 - \left|\left(\frac{c\lambda^2 U_0}{1 - M_2}\right)\right|^2. \quad (54)$$

Δ depends mainly upon the non-dimensional frequencies, κa and ka, and only weakly upon the diameter ratio, λ. It is convenient to have just one frequency-dependent variable, the Strouhal number, $\mathrm{St}_a = fa/\bar{u}_1$, where f is the frequency in Hertz and $\bar{u}_1$ is the upstream mean flow velocity. The results can then be expressed in terms of the Strouhal number, St_a, the Mach number, $M_1 = \bar{u}_1/c$, and the diameter ratio λ.

Figure 2 shows the calculated acoustic absorption coefficient for two joint semi-infinite pipes, as a function of the Strouhal number over a range of Mach numbers and for $\lambda = 0{\cdot}73$. It is clear that a significant fraction of the incident energy can be absorbed by this mechanism. Note that, for this value of λ and the range of Mach numbers considered, the maximum acoustic absorption occurs at almost a constant Strouhal number of about 2. There is negligible acoustic absorption for low and high Strouhal numbers. This

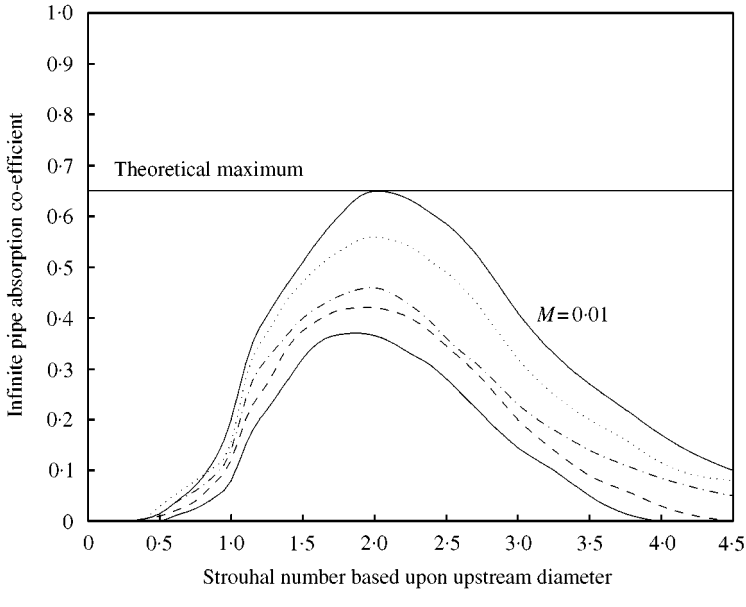

Figure 2. Acoustic absorption coefficient for two semi-infinite pipes, $\lambda = 0{\cdot}733$ ⋯, $M = 0{\cdot}015$; – –, $M = 0{\cdot}025$; ——, $M = 0{\cdot}05$; —, $M = 0{\cdot}1$.

low-frequency behaviour may appear, at first sight, to contradict the work of Bechert *et al.* [43], who find significant "absorption" at vanishingly low frequencies. The discrepancy can be explained, however, by noting the different definition of the acoustic absorption coefficient used by Bechert *et al.* In their results, the absorbed sound is normalized on the net sound flowing down the pipe (which tends to zero at low frequencies) rather than on the incident sound energy as here. Thus at very low frequencies, small acoustic absorption appears large because of the very small denominator. When their results are renormalized to give an acoustic absorption coefficient defined in the same way as here, they too find negligible low-frequency sound absorption, for low Mach number flow.

By differentiating equation (54) with respect to U_0, one finds an overall maximum acoustic absorption, by any mechanism, Δ_{opt}, of $1/(1 + \lambda^2)$. It is clearly seen in the numerical results, displayed in Figure 2, that Δ_{opt} is nearly achieved at a Mach number of 0·01; a reasonable Mach number in liquids, but low in air. Even at a Mach number of 0·1, however, a significant amount of acoustic absorption (the maximum is 0·38) is achieved.

The variation of the acoustic absorption with the diameter ratio, λ is shown in Figures 3 and 4. Figure 3 shows the calculated acoustic absorption coefficient, Δ, as function of Strouhal number, St_a, for a fixed Mach number and varying diameter ratio, λ; whilst Figure 4 shows the Strouhal number for maximum acoustic absorption, $\mathrm{St}_{a,max}$, as a function of the diameter ratio, λ. For large expansion ratios, i.e., for low values of $\lambda (< 0{\cdot}35)$, the optimum Strouhal number is virtually independent of λ and fixed at approximately 1. This occurs because the walls of the second pipe have very little effect upon the local behaviour near the expansion lip, when the expansion ratio is large.

In contrast, for small area changes, i.e., large values of $\lambda (\geqslant 0{\cdot}65)$, the Strouhal number for maximum acoustic absorption, $\mathrm{St}_{a,max}$, varies greatly with λ because the wall of the second pipe has a large effect upon the local behaviour near the expansion lip and hence upon the vortex shedding. Under such circumstances the relevant length scale is no longer the diameter of the smaller pipe, but the step height, $h = b - a$. It is therefore appropriate to use a different Strouhal number based on the step height, h, rather than upon the smaller

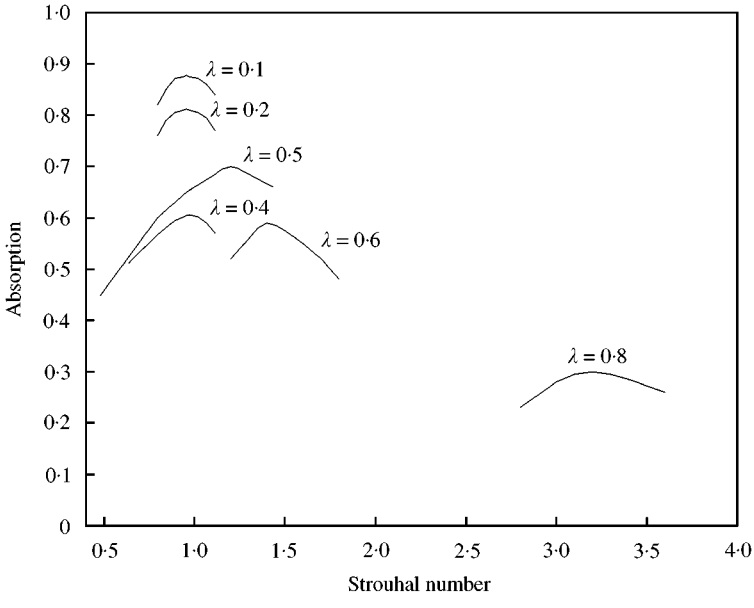

Figure 3. The variation of Δ with St_a with varying λ.

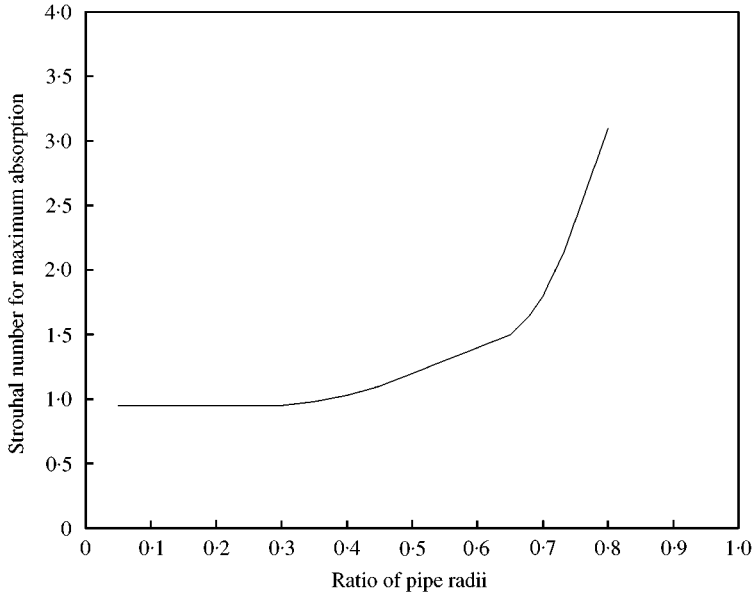

Figure 4. The variation of $St_{a,max}$ with λ, $M_1 = 0{\cdot}025$.

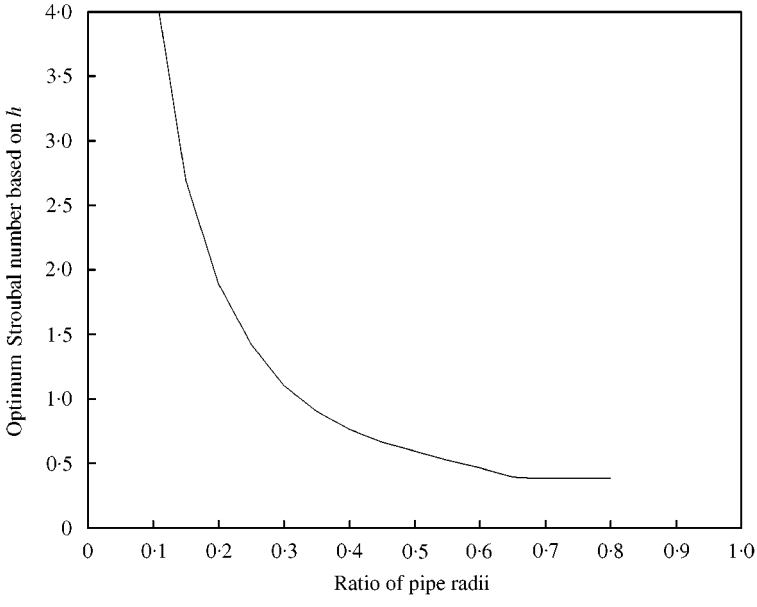

Figure 5. The variation of $St_{h,max}$ with λ, $M_1 = 0{\cdot}025$.

pipe radius, a, to give St_h, with the Strouhal number for optimum acoustic absorption occurring at $St_{h,max}$. Thus Figure 4 is replotted as a function of $St_{h,max}$ instead of $St_{a,max}$. The results are shown in Figure 5 where it is seen that the Strouhal number for maximum acoustic absorption based upon step height, $St_{h,max}$, is virtually independent of λ and fixed at about 0·4 for large values of λ.

3. THE EFFECT OF PIPE RESONANCES

Consider now the more realistic problem of propagation of acoustic waves past a sudden axisymmetric area expansion with flow in pipes of finite length. Just as for the two-dimensional problem described in Dupère and Dowling [36, 37], the conversion of sound waves into vortical motion, and hence the acoustic absorption, is dramatically enhanced near pipe resonances. The analysis follows very similar lines to that presented in that paper, with reflection from the pipe ends leading to waves in both pipes incident on the area change. As for the two-dimensional problem, the additional incoming sound wave has a linear effect upon the forcing term at $x = 0$.

To illustrate the effects of pipe resonances, consider the particular geometry illustrated in Figure 6: an open-ended pipe of radius a and effective length L is connected coaxially to a larger diameter pipe of radius b to form a sudden area expansion at $x = 0$. As before there is a mean flow from the smaller to the larger diameter pipe. An incoming plane sound wave of amplitude C_0 propagates in the negative x-direction towards the area change at $x = 0$. At the area change the sound wave is partly reflected and partly transmitted into the smaller pipe where it propagates in the negative x-direction towards the open end and is reflected giving a second incident sound were propagating in the positive x-direction from the open end (at $x = -L$) towards the area change at $x = 0$. The (complex) amplitude of this second incident sound wave is denoted by B_0 as shown in Figure 6. For sufficiently long pipe lengths, L, and for sufficiently low frequency, this second incident sound wave will also be planar. As with semi-infinite pipes, the perturbations in $x < 0$ satisfy equation (14):

$$B(x, r_0) = B_0 e^{ikx/(1+M_1)} + B_0 e^{-ikx/(1-M_1)} + \int_0^a i2\pi f \bar{G}_1 U(r_0) r_0 \, dr_0 \tag{55}$$

whilst equation (26) must be modified to take account of the incident sound wave, C_0:

$$B(x, r) + C_0 e^{ikx/(1+M_2)} + C_0 e^{-ikx/(1-M_2)} + \sigma S(x, r) = -i2\pi f \int_0^a \bar{G}_2 U(r_0) r_0 \, dr_0. \tag{56}$$

As before $U(r)$ and σ are to be determined by applying the condition that $B(x, r)$ is continuous across $x = 0$ for $r \leqslant a$ and by applying the Kutta condition at $x = 0$ and $r = a$. This leads to an equation which is entirely equivalent to equation (26) save that the forcing term B_0 is now replaced by $(B_0 - C_0)$, where B_0 and C_0 are both complex. This equivalence can be exploited by using an expansion

$$U(r_0) = (B_0 - C_0) \sum_{m=0}^{\infty} U_m J_0(j_m r/a) \tag{57}$$

in place of equation (45). The coefficients U_m, $m = 0, 1, 2, \ldots$, are identical to those already calculated for the semi-infinite pipes. The significance of this is that the solution for any

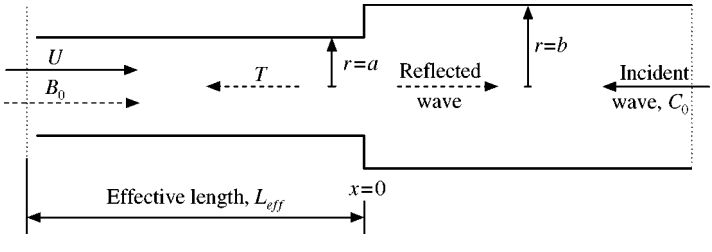

Figure 6. Finite pipe geometry.

number of different lengths of pipe (as functions of Mach number, M; Strouhal number, St_a; and diameter ratio, λ) can be derived from the single calculation for the semi-infinite pipes (again as a function of M, St_a and λ) provided the ratio B_0/C_0 is known. It will now be shown that this just requires knowledge of the reflection coefficient at $x = -L$. Define this reflection coefficient, R_L, by $B_0 = R_L T \mathrm{e}^{2\mathrm{i}kL}$, where T is the transmitted wave travelling from right to left in the smaller diameter pipe as shown in Figure 6, and R_L is the reflection coefficient and L is the length of the smaller diameter pipe in $x < 0$, as shown in Figure 6. The ratio B_0/C_0 is determined by applying this reflection coefficient at the open end of the smaller diameter pipe. In the upstream region away from the junction between the pipes, any high order modes are exponentially small and the remaining plane waves are described by a modified form of equation (47):

$$B(x) = B_0 \mathrm{e}^{\mathrm{i}kx(1+M_1)} + \mathrm{e}^{-\mathrm{i}kx(1-M_1)}\left(B_0 - (B_0 - C_0)\left(\frac{cU_0}{1+M_1}\right)\right) \quad \text{for } x \ll 0. \tag{58}$$

Using this form for B and the reflection coefficient at $x = -L$ leads to a second equation relating B_0 and C_0:

$$B_0 = R_L \mathrm{e}^{2\mathrm{i}kL}\left(B_0 - (B_0 - C_0)\left(\frac{cU_0}{1+M_1}\right)\right). \tag{59}$$

Equation (59) is solved to show that

$$\frac{B_0 - C_0}{C_0} = -\frac{1 - R_L \mathrm{e}^{2\mathrm{i}kL}}{1 - R_L \mathrm{e}^{2\mathrm{i}kL} + R_L \mathrm{e}^{2\mathrm{i}kL}(cU_0/(1+M_1))}. \tag{60}$$

The reflection coefficient is to be determined by consideration of the type of end correction at $x = -L$, either theoretically or by experiment. For large positive x, equation (56) simplifies to

$$B(x) = C_0 \mathrm{e}^{-\mathrm{i}kx/(1-M_2)} + \left(C_0 + (B_0 - C_0)\left(\frac{cU_0\lambda^2}{1-M_2}\right)\right)\mathrm{e}^{\mathrm{i}kx/(1+M_2)} \quad \text{for } x \gg 0 \tag{61}$$

(cf. equation (48)), and the proportion of incident sound energy which is absorbed is

$$\Delta_L = 1 - \left(\frac{|B_0/C_0 - ((B_0 - C_0)/C_0)(cU_0/(1+M_1))|^2}{|B_0/C_0|^2\lambda^2 + 1}\lambda^2\right) - \left(\frac{|1 - ((B_0 - C_0)/C_0)(cU_0\lambda^2/(1-M_2))C_0^2|^2}{|B_0/C_0|^2\lambda^2 + 1}\right), \tag{62}$$

where $(B_0 - C_0)/C_0$ and B_0/C_0 are determined from equation (60) for a known complex value of R_L.

The unknown, U_0, is determined from the semi-infinite pipe calculations and thus equation (62) can be used to predict the acoustic absorption coefficient for pipes of any length, L, and Mach number, M_1, provided the reflection coefficient at the inlet, R_L, is known.

4. EXPERIMENTAL WORK

The basic layout of the experimental rig is illustrated in Figure 7 which is not drawn to scale. Ambient air enters a 0·18 m straight cylindrical pipe of internal diameter 96 mm

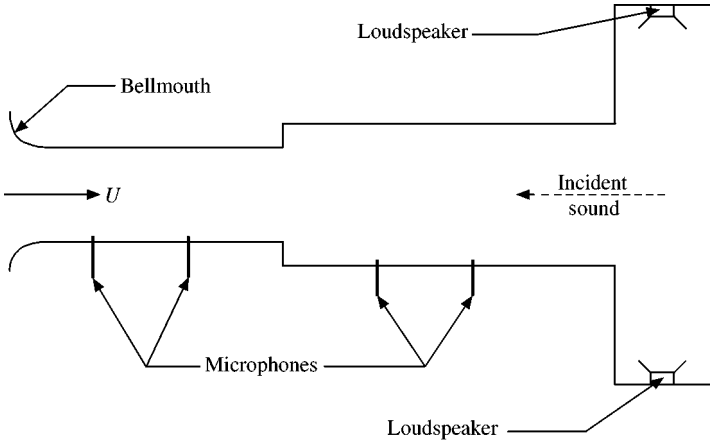

Figure 7. Experimental layout.

through a smooth bellmouth. There is an abrupt area expansion into a second coaxial, cylindrical pipe of internal diameter 130 mm and length 0·2 m. This second pipe exhausts into a $1{\cdot}82 \times 1{\cdot}21 \times 1{\cdot}21\,\mathrm{m}^3$ plenum chamber which in turn is connected to an axial blower. The mean flow velocity is measured at the inlet using a hot wire to an accuracy of 3%.

In the presented theory, the square of the mean flow Mach number is assumed small in comparison with unity. In the experiment the mean flow Mach number (in the smaller pipe) is varied from 0·015 to 0·1 (which is the largest Mach number obtainable with this arrangement) and so such effects may certainly be ignored. The theory also requires that the Stokes layer be thin in comparison with the mean shear layer. Over the experimental velocity range the mean boundary layer thickness just upstream of the expansion is estimated to be at least 16% of the smaller pipe radius. The thickness of the Stokes layer, $(\nu/\pi f)^{1/2}$, describing the unsteady shear layer, on the other hand, is estimated to be at most 0·5 mm (for a frequency of 100 Hz, the lowest frequency of interest). Hence, the unsteady shear layer is thinner than the mean shear layer by at least a factor of 0·06. Finally, the additional condition for the neglect of the mean vorticity term requires that the Strouhal number be larger than approximately 0·2, which is achieved here.

Pressure waves are generated by an arrangement of four loudspeakers in the plenum chamber (two of which are shown in Figure 7) providing an incident sound wave propagating towards the expansion from right to left in Figure 7. The loudspeakers are excited at a single frequency, which is chosen to be sufficiently low that only the plane wave propagates, i.e., so that $kb < j_1 = 3{\cdot}832$. This restricts the frequency range to frequencies below 3·3 kHz. In order to ensure that the higher order modes decay sufficiently rapidly away form the ends of the pipe, however, a practical limit of 1 kHz is taken. This gives 20 dB decay over an axial distance of 50 mm in the larger pipe and within 30 mm in the smaller pipe for the first ($n = 1$) mode. Higher modes decay even more rapidly. The Strouhal number range given by this constraint is for Strouhal numbers, $\mathrm{St}_a = fa/\bar{u}_1$, less than 10 for the mean flow rates considered.

Measurements of the pressure waves in the two pipes are obtained by a technique based upon the two microphone method [44, 45]. As in the two-dimensional paper [36, 37], a microphone spacing of 0·1 m is chosen. The microphones are symmetrically positioned within the pipes (i.e., 4 cm from each end in the smaller diameter pipe, and 5 cm from each end in the larger diameter pipe) and are thus sufficiently far from the ends of the pipes to

ensure that the non-planar wave modes (for which $n > 0$) are attenuated by at least 25 dB compared with their values at the pipe ends. Here the two microphone technique is simplified because only one frequency waves are propagating and, thus the waves are found by simply solving a small set of simultaneous equations involving the complex pressure signals (magnitude and phase). The calibration procedure is the same as described in our earlier paper [36, 37] in which the microphones were placed very close to each other in a box and used to measure the same known signal. The phase difference between the two microphones, determined by the calibration procedure was found to be approximately 4°, depending slightly on the frequency, but was found to be repeatable. This gives a maximum error in the measured amplitudes of 7% which occurs at small values of the acoustic absorption coefficient. The results show that the acoustic absorption coefficient is significant at most frequencies and so the error in the amplitude is considerably less.

The experimental procedure is as follows. First, the two microphones are calibrated relative to each other. Next, the two microphones in the smaller diameter pipe are used to determine the reflection coefficient of the bellmouth at the open end of the pipe. The signals obtained from the microphones are filtered using anti-aliasing filters with a cut-off frequency of 4 kHz and samples taken for 2 s giving a resolution of 0·5 Hz. The sound waves in the positive and negative x-directions are then obtained by solving the simultaneous equations as described above.

First, the reflection coefficient, R_L, for the bellmouth at the open end of the pipe was deduced as a function of frequency (and hence of Strouhal number). Figure 8 shows results for the magnitude of R_L as a function of the Strouhal number from which it is clear that, for Strouhal numbers greater than 0·4, the magnitude of the reflection coefficient, R_L, is constant and unity. Results for the phase of the reflection coefficient can be expressed in terms of an end correction:

$$\text{phase } R_L = \pi + 2k\delta.$$

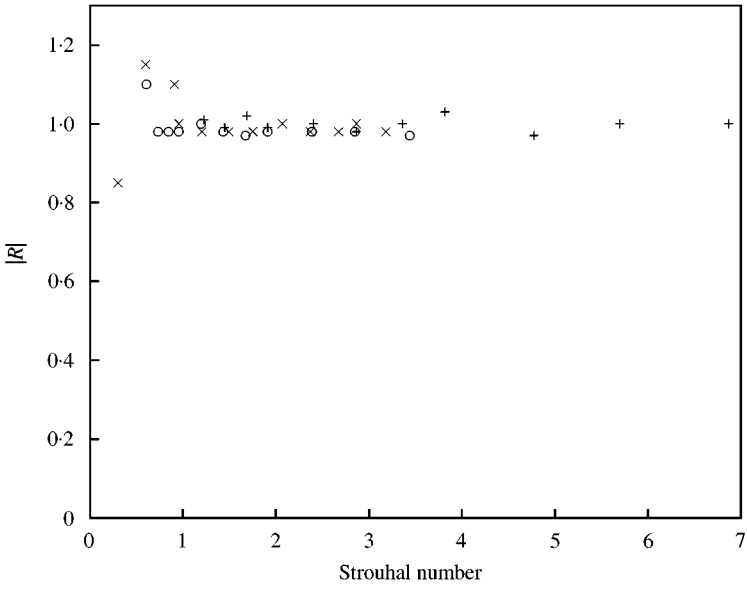

Figure 8. The magnitude of the reflection coefficient as a function of St_a; ×, $M_1 = 0{\cdot}05$; ○, $M_1 = 0{\cdot}025$; +, $M_1 = 0{\cdot}015$.

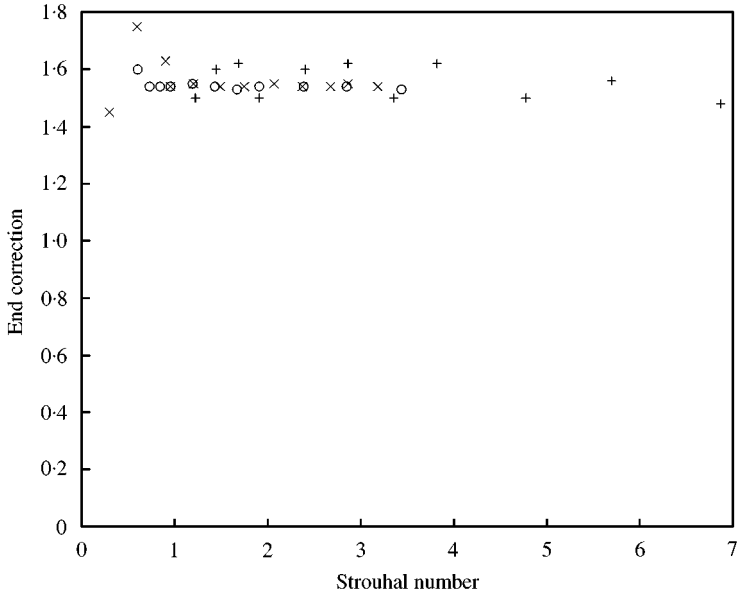

Figure 9. The measured end corrections as a function of St_a; ×, $M_1 = 0{\cdot}05$; ○, $M_1 = 0{\cdot}025$; +, $M_1 = 0{\cdot}015$.

Figure 9 shows the measured values of the end correction, based on a correction to the length of the straight portion of the pipe, as a function of the Strouhal number. It is clear that, for $\mathrm{St}_a > 0{\cdot}4$, δ is approximately constant at $1.55a$. This differs from the familiar straight pipe open end correction, $\delta \approx 0{\cdot}6a$ [19] because of the presence of the bellmouth, the mean flow having little effect at such high Strouhal numbers in agreement with Peters *et al.* [27]. The experimental reflection coefficient can therefore be expressed in the form $R_L = -\mathrm{e}^{2\mathrm{i}k\delta}$. After substitution into equation (62), this leads to a theoretical prediction for the sound absorption:

$$\Delta_L = 1 - \left| 1 + \left(\frac{1 + M_1}{1 - M_2} \right) \left(\frac{2\cos(kL_{eff}) c\lambda^2 U_0}{2\cos(kL_{eff})(1 + M_1) - \mathrm{e}^{\mathrm{i}kL_{eff}} c U_0} \right) \right|^2, \tag{63}$$

where $L_{eff} = L + \delta$ is the effective length of the smaller diameter pipe. This is to be compared with measurement.

In the large pipe two microphones are used to determine the stagnation enthalpy reflection coefficient, $R_a = (\text{reflected wave})/C_0$, of the incident sound wave on the area change. The acoustic absorption coefficient, Δ_L, is defined to be the sound energy absorbed as a fraction of the incident sound energy in the larger pipe:

$$\Delta_L = 1 - |R_a|^2. \tag{64}$$

There is no net energy flux in the smaller pipe with the open end.

In taking the readings due care was taken to ensure that the readings lie in the linear regime. To test for linearity, the amplitude of the sound emitted from the loudspeakers is varied and new measurements are taken. Throughout the linear regime all pressure measurements increase in proportion to one another and, hence, the acoustic absorption coefficient, Δ_L, is independent of incident sound wave amplitude.

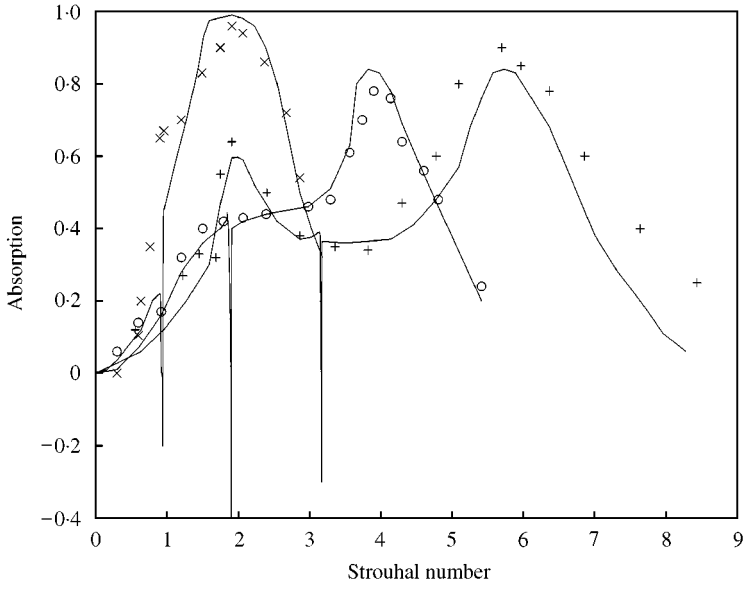

Figure 10. Δ_L, as a function of St_a, for $\lambda = 0{\cdot}73$, and a range of Mach numbers: — analytical; ×, $M_1 = 0{\cdot}05$ experimental reading; ○, $M_1 = 0{\cdot}025$ experimental reading; +, $M_1 = 0{\cdot}015$ experimental reading.

Figure 10 shows the calculated and measured acoustic absorption coefficient, Δ_L, as a function of the Strouhal number based upon the upstream diameter, $\mathrm{St}_a = fa/\bar{u}_1$, for a fixed value of the diameter ratio, $\lambda = 0{\cdot}73$, and a range of Mach numbers. The agreement between the predictions and the experimental measurements is encouraging. In particular, the frequency for peak acoustic absorption is very well predicted for all three Mach numbers tested. The amplitude of the peak acoustic absorption is also predicted to within 8%.

It is clear that the finite length acoustic absorption coefficient, Δ_L, has, in general, two local maxima. First, maxima occur at frequencies corresponding to half-wavelength resonances of the smaller pipe, giving rise to greatly enhanced acoustic absorption. Since these frequencies are relatively independent of Mach number, this is more clearly seen in Figure 11 where the finite length acoustic absorption coefficient, Δ_L, is replotted as a function of kL. At the resonance frequency, $kL = \pi$, the forcing term, $(B_0 - C_0)$, in equation (60) becomes maximum and so the strength of the shed vorticity becomes large giving rise to very effective sound absorption. Conversely, when the frequency corresponds to a quarter wavelength resonance in the first pipe, the forcing term, $(B_0 - C_0)$, becomes zero, resulting in zero acoustic absorption, which subsequently becomes briefly negative. This occurs, however, over a very narrow frequency range as a result of the large semi-infinite pipe acoustic absorption and so, although predicted by the theory, it is not observed in the experimental results. The effects of both quarter and half-wavelength resonance were also noted in the 2-D problem [36, 37]. In that problem, however, the infinite pipe acoustic absorption was much less. As a result, small acoustic absorption near quarter-wavelength resonances was observed in the experiment as well as in the theory.

At the Mach numbers described in this paper, the infinite pipe results have a distinct peak (at a Strouhal number of about 2). This gives rise to a second type of maxima, corresponding to the maximum acoustic absorption for semi-infinite pipes. Since one maximum is a function of the speed of sound, and one a function of the flow speed, it is possible for both

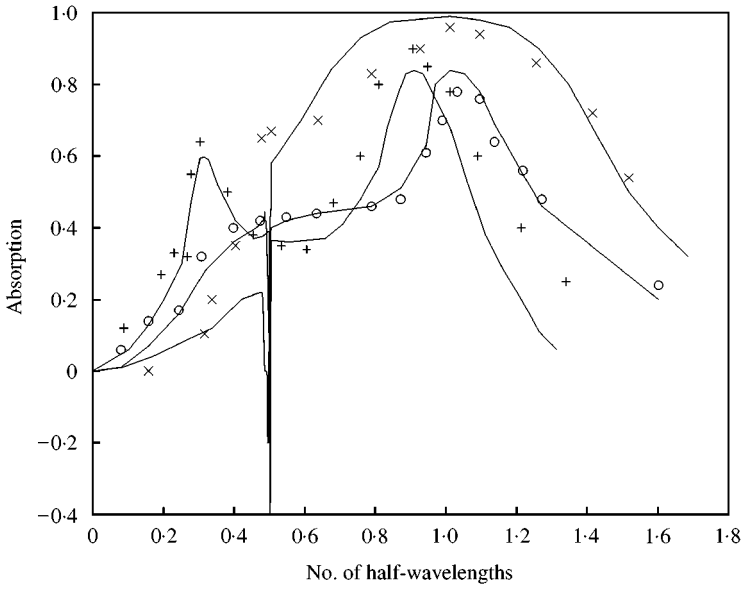

Figure 11. Δ_L, as a function of kL, for $\lambda = 0{\cdot}73$, and a range of Mach number: — analytical; ×, $M_1 = 0{\cdot}05$ experimental reading; ○, $M_1 = 0{\cdot}025$ experimental reading; +, $M_1 = 0{\cdot}015$ experimental reading.

to coincide. This occurs when the pipe resonance, $kL = \pi$, is at a Strouhal number based upon the upstream radius of 2, i.e., when

$$M = (\tfrac{1}{4})\, a/L. \tag{65}$$

For the geometry used in Figures 10 and 11, $a/L = 0{\cdot}2$ and this corresponds to a Mach number of 0·05. The results for this Mach number are included in Figures 10 and 11 where it is clear that there is only one maximum and it corresponds to almost total acoustic absorption, $\Delta_L = 1$. Thus, the best acoustic absorption is achieved by arranging for the pipe resonance to occur at the Strouhal number for maximum acoustic absorption in semi-infinite pipes.

5. CONCLUSIONS

This paper has shown how an acoustic analogy can be applied along with a very simple model for the shed vorticity to accurately predict the sound absorption by flow/sound interaction across a sudden area expansion in axisymmetic pipes.

The magnitude of the diameter ratio, $\lambda = a/b$, affects the appropriate length scale to be used in the definition of the Strouhal number. For small expansion ratios, i.e., $\lambda \geqslant 0{\cdot}65$ the appropriate Strouhal number of St_h based upon the step height $h = b - a$. For large expansion ratios, $\lambda \leqslant 0{\cdot}3$ the image sources have little effect and the appropriate Strouhal number is St_a based upon the smaller pipe radius a, the optimum occurring at an approximately constant value of about 2. For intermediate values of λ, the optimum Strouhal number is found to depend upon λ. The maximum acoustic absorption depends upon both the Mach number, M, and the diameter ratio, λ.

With sound waves incident from both directions, both far upstream and far downstream, the conversion of sound energy into unsteady vortical motion can be either enhanced or

suppressed, depending upon the relative magnitude and phase of incoming soundwaves. Two maxima occur in the finite pipe case: one related to the Strouhal number for maximum acoustic absorption in semi-infinite pipes, and the other related to half-wavelength pipe resonance. By suitable choice of Mach number for this geometry (or indeed by suitable choice of geometry for a given Mach number) it is possible to arrange for both these maxima to coincide resulting in very high levels of acoustic absorption (almost total acoustic absorption for this geometry and a Mach number of 0·05).

REFERENCES

1. M. J. LIGHTHILL 1952 *Proceedings of the Royal Society of London* **A211**, 564–587. On sound generated aerodynamically. I. General theory.
2. M. J. LIGHTHILL 1974 *Proceedings of the Royal Society of London* **A222**, 1–32. On sound generated aerodynamically. II. Turbulence as a source of sound.
3. A. POWELL 1964 *Journal of the Acoustical Society of America* **36**, 177–195. Theory of vortex sound.
4. M. S. HOWE 1975 *Journal of Fluid Mechanics* **71**, 625–673. Contributions to the theory of aerodynamic sound, with application to excess jet noise and the theory of the flute.
5. P. E. DOAK 1989 *Journal of Sound and Vibration* **131**, 67–90. Momentum potential-theory of energy flux carried by momentum fluctuations.
6. P. E. DOAK 1995 *Acoustical Physics* **41**, 677–685. Fluctuating total enthalpy as a generalised acoustic field.
7. P. E. DOAK 1996 *Acoustical Physics* **42**, 650. Errata to fluctuating total enthalpy as a generalised acoustic field (**41**, 677–685).
8. P. E. DOAK 1998 *Theoretical and Computational Fluid Dynamics*, *Special Volume in Honor of Sir James Lighthill* **10**, 115–133. Fluctuating total enthalpy as the basic generalised acoustic field.
9. D. W. BECHERT 1980 *Journal of Sound and Vibration* **70**, 389–405. Sound absorption caused by vorticity shedding, demonstrated with a jet flow.
10. W. BORTH 1916 *Zeitschrift des VDI* **60**, 565–569. Vibration and resonance phenomena in the ducts of piston compressors.
11. U. V. INGARD and S. LABATE 1950 *Journal of the Acoustical Society of America* **22**, 211–218. Acoustic circulation effects and nonlinear impedance of orifices.
12. U. V. INGARD and H. ISING 1967 *Journal of the Acoustical Society of America* **42**, 6–17. Acoustic nonlinearity of an orifice.
13. A. CUMMINGS 1984 *American Institute of Aeronautics and Astronautics Journal* **22**, 786–792. Acoustic nonlinearities and power losses at orifices.
14. A. CUMMINGS 1984 *Technical Report* 84-2311, *American Institute of Aeronautics and Astronautics*. Transient and multiple frequency sound transmission through perforated plates at high amplitude.
15. M. S. HOWE 1979 *Proceedings of the Royal Society of London* **A366**, 205–223. On the theory of unsteady high Reynolds number flow through a circular aperture.
16. I. J. HUGHES and A. P. DOWLING 1990 *Journal of Fluid Mechanics* **218**, 299–335. The absorption of sound by perforated linings.
17. M. S. HOWE 1980 *Proceedings of the Royal Society of London* **A370**, 523–544. On the diffraction of sound by a screen with circular apertures in the presence of a low Mach number grazing flow.
18. G. F. CARRIER 1956 *Quarterly of Applied Mathematics* **13**, 457–461. Sound transmission from a tube with flow.
19. H. LEVINE and J. SCHWINGER 1948 *Physical Review* **73**, 386–406. On the radiation of sound from an unflanged circular pipe.
20. S. D. SAVKAR 1975 *Journal of Sound and Vibration* **42**, 363–386. Radiation of cylindrical duct modes with flow mismatch.
21. R. M. MUNT 1977 *Journal of Fluid Mechanics* **83**, 609–640. The interaction of sound with a subsonic jet issuing from a semi-infinite cylindrical pipe.
22. R. M. MUNT 1990 *Journal of Sound and Vibration* **142**, 413–436. Acoustic transmission properties of a jet pipe with subsonic jet flow. I. The cold jet reflection coefficient.
23. A. M. CARGILL 1982 *Journal of Fluid Mechanics* **121**, 59–105. Low frequency sound radiation and generation due to the interaction of unsteady flow with a jet pipe.

24. A. M. CARGILL 1982 *Journal of Sound and Vibration* **83**, 339–354. Low frequency acoustic radiation from a jet pipe—a second order theory.
25. S. W. RIENSTRA 1981 *Trans ASME Journal of Engineering for Industry* **103**, 378–384. On the acoustical implications of vortex shedding from an exhaust pipe.
26. S. W. RIENSTRA 1983 *Journal of Sound and Vibration* **86**, 539–556. A small Strouhal number analysis for acoustic wave-jet flow-pipe interaction.
27. M. C. A. M. PETERS, A. HIRSHBERG, A. J. RIJNEN and A. P. J. WIJNANDS 1993 *Journal of Fluid Mechanics* **256**, 499–534. Damping and reflection measurements for an open pipe at low Mach and low Helmholtz numbers.
28. P. O. A. L. DAVIES, J. L. BENTO COELHO and M. BHATTACHARYA 1980 *Journal of Sound and Vibration* **72**, 543–546. Reflection coefficient for an unflanged pipe with flow.
29. M. S. HOWE 1979 *Journal of Fluid Mechanics* **91**, 209–229. Attenuation of sound in a low Mach number nozzle flow.
30. I. L. VÉR 1990 *Noise Control Engineering Journal* **35**, 115–125. Practical examples of noise and vibration: case history of consulting projects.
31. M. S. HOWE 1980 *Journal of Fluid Mechanics* **97**, 641–653. The influence of vortex shedding on the diffraction of sound by a perforated screen.
32. Y. FUKUMOTO and M. TAKAYANA 1991 *Physics of Fluids* **A3**, 3080–3082. Vorticity production at the edge of a slit by sound waves in the presence of a low Mach number bias flow.
33. A. P. DOWLING and I. J. HUGHES 1992 *Journal of Sound and Vibration* **156**, 387–405. Sound absorption by a screen perforated with a regular array of slits.
34. P. A. NELSON, N. A. HALLIWELL and P. E. DOAK 1981 *Journal of Sound and Vibration* **78**, 15–38. Fluid dynamics of a flow excited resonance. Part I: Experiment.
35. P. A. NELSON, N. A. HALLIWELL and P. E. DOAK 1983 *Journal of Sound and Vibration* **91**, 375–402. Fluid dynamics of a flow excited resonance. Part II: Flow acoustic interaction.
36. I. D. J. DUPÈRE and A. P. DOWLING 1998 *Technical Report* 98-2303, *Proceedings of the* 4*th AIAA/CEAS Aeroacoustics Conference*, *Toulouse*, *France*. The absorption of sound near abrupt area expansions.
37. I. D. J. DUPÈRE and A. P. DOWLING 2000 *American Institute of Aeronautics and Astronautics Journal* **38**, 193–202. The absorption of sound near abrupt area expansions.
38. D. G. CRIGHTON 1985 *Annual Review of Fluid Mechanics* **17**, 411–445. The Kutta condition in unsteady flow.
39. P. G. DANIELS 1978 *Quarterly Journal of Mechanics and Applied Mathematics* **31**, 49–75. On the unsteady Kutta condition.
40. J. C. WENDOLOSKI. Private communication.
41. M. ABRAMOWITZ and I. A. STEGUN 1965 *Handbook of Mathematical Functions*. New York: Dover Publications.
42. C. L. MORFEY 1971 *Journal of Sound and Vibration* **14**, 37–55. Sound transmission and generation in ducts with flow.
43. W. D. BECHERT, U. MICHEL and E. PFIZENMAIER 1978. *American Institute of Aeronautics and Astronautics Journal* **16**, 873–874. Experiments on the transmission of sound through jets.
44. A. F. SEYBERT and D. F. ROSS 1977 *Journal of the Acoustical Society of America* **61**, 1362–1370. Experimental determination of acoustic properties using a two microphone random excitation technique.
45. A. F. SEYBERT and B. SOENARKO 1981 *Journal of the Acoustical Society of America* **69**, 1190–1199. Error analysis of spectral estimates with application to the measurement of acoustic parameters using random sound fields in ducts.